JBC RESEARCH ARTICLE

Intracerebroventricular dosing of N-sulfoglucosamine sulfohydrolase in mucopolysaccharidosis IIIA mice reduces markers of brain lysosomal dysfunction

Received for publication, February 16, 2022, and in revised form, October 15, 2022 Published, Papers in Press, October 26, 2022,
https://doi.org/10.1016/j.jbc.2022.102625

Jenna Magat[1], Samantha Jones[1], Brian Baridon[1], Vishal Agrawal[1], Hio Wong[2], Alexander Giaramita[1], Linley Mangini[1], Britta Handyside[1], Catherine Vitelli[1], Monica Parker[2], Natasha Yeung[2], Yu Zhou[2], Erno Pungor[2], Ilya Slabodkin[1], Olivia Gorostiza[1], Allora Aguilera[2], Melanie J. Lo[1], Saida Alcozie[1], Terri M. Christianson[1], Pascale M. N. Tiger[1], Jon Vincelette[1], Sylvia Fong[1], Geuncheol Gil[2], Chuck Hague[2], Roger Lawrence[1], Daniel J. Wendt[1], Jonathan H. Lebowitz[1], Stuart Bunting[1], Sherry Bullens[1], Brett E. Crawford[1], Sushmita M. Roy[2], and Josh C. Woloszynek[1,*]

From the [1]Department of Research, BioMarin Pharmaceutical Inc, Novato, California, USA; [2]Department of Process Sciences, BioMarin Pharmaceutical Inc, Novato, California, USA

Edited by Ronald Wek

Mucopolysaccharidosis type IIIA (MPS IIIA) is a lysosomal storage disorder caused by N-sulfoglucosamine sulfohydrolase (SGSH) deficiency. SGSH removes the sulfate from N-sulfoglucosamine residues on the nonreducing end of heparan sulfate (HS-NRE) within lysosomes. Enzyme deficiency results in accumulation of partially degraded HS within lysosomes throughout the body, leading to a progressive severe neurological disease. Enzyme replacement therapy has been proposed, but further evaluation of the treatment strategy is needed. Here, we used Chinese hamster ovary cells to produce a highly soluble and fully active recombinant human sulfamidase (rhSGSH). We discovered that rhSGSH utilizes both the CI-MPR and LRP1 receptors for uptake into patient fibroblasts. A single intracerebroventricular (ICV) injection of rhSGSH in MPS IIIA mice resulted in a tissue half-life of 9 days and widespread distribution throughout the brain. Following a single ICV dose, both total HS and the MPS IIIA disease-specific HS-NRE were dramatically reduced, reaching a nadir 2 weeks post dose. The durability of effect for reduction of both substrate and protein markers of lysosomal dysfunction and a neuroimmune response lasted through the 56 days tested. Furthermore, seven weekly 148 μg doses ICV reduced those markers to near normal and produced a 99.5% reduction in HS-NRE levels. A pilot study utilizing every other week dosing in two animals supports further evaluation of less frequent dosing. Finally, our dose–response study also suggests lower doses may be efficacious. Our findings show that rhSGSH can normalize lysosomal HS storage and markers of a neuroimmune response when delivered ICV.

Mucopolysaccharidosis Type IIIA (MPS IIIA, Sanfilippo Syndrome Type A) is an autosomal recessive lysosomal storage disease caused by mutations in the gene encoding the enzyme N-sulfoglucosamine sulfohydrolase (SGSH, sulfamidase, EC 3.10.1.1). Deficiency of SGSH activity results in the progressive lysosomal accumulation of partially degraded heparan sulfate (HS) glycosaminoglycans, with disease specific N-sulfoglucosamine on the nonreducing end (HS-NRE), in the brain and peripheral organs (1). This lysosomal storage results in hepatosplenomegaly, respiratory infections, and progressive neurologic dysfunction in the brain. Patients typically present with missed developmental milestones such as the onset of speech, alterations in sleep, and behavioral challenges. As the neurological disease progresses, the attainment of developmental abilities plateaus and subsequently declines as regions of atrophy in the brain expand. The disease progression varies across a wide spectrum, with the most severe patients succumbing to death by the second decade of life while the mildest patients may survive into their sixth decade of life (2–4). While it is unclear how lysosomal storage manifests into the highly variable clinical phenotype of Sanfilippo Syndrome, which consists of four genetically and biochemically distinct MPS III syndromes (types A, B, C, and D), the profound central nervous system (CNS) presentation with moderate peripheral disease manifestations highlights the common HS fragments as potential drivers of clinical pathology (1, 5). Currently, this pathology in MPS IIIA patients is only treated with palliative care as there are no approved disease modifying therapies.

The amount of stored lysosomal HS that is still conducive to normal cellular function is unknown. Thus, the ideal therapy for MPS IIIA would restore sufficient sulfamidase enzymatic activity to normalize HS degradation throughout the body. Preclinical therapeutic attempts to intervene in MPS IIIA have aimed to replace the missing enzyme directly with recombinant human SGSH (rhSGSH) or indirectly through gene therapy. Utilizing either strategy, the treatment has been administered to the brain directly or to the periphery with the hope that enough enzymes will cross the blood–brain barrier. rhSGSH enzyme replacement therapy (ERT) directly to the CNS has been evaluated previously in mice (6–11) and dogs

* For correspondence: Josh C. Woloszynek, josh.woloszynek@gmail.com.

(12–14). Gene therapies have also been delivered directly to the CNS or administered peripherally in mice (15–21) and humans (22). In the case of peripheral administration, strategies have been employed to extend the pharmacokinetics of the enzyme in the blood (23) or enhance brain uptake through a peptide tag binding to brain transporters (24). Direct comparison of the effectiveness of the different preclinical treatment approaches is difficult due to the variety, specificity, and sensitivity of the analytical tools used to measure HS (25). In MPS IIIA patients, these approaches have failed to normalize cerebrospinal fluid (CSF) HS or halt cognitive decline (22, 26, 27). While storage was reduced both preclinically and clinically, the failure to normalize indicates biochemical inadequacy and potentially allows for continued disease progression. Although substantial reductions in CSF HS were expected to alter the disease course, complicating factors affecting this interpretation include the noted device failures and the age of the patients at the start of treatment (5, 26, 27). While previously published preclinical MPS IIIA ERT studies suggest that higher doses of enzyme frequently delivered intracerebroventricular (ICV) might normalize lysosomal storage in the brain, similar to what is seen with MPS IIIB, the age of treatment onset is also likely a critical component (28).

In order to properly interpret ERT biodistribution and substrate clearance results, a thorough understanding of cellular uptake mechanisms is necessary. Many lysosomal enzymes can traffic from the extracellular space to the lysosome by the binding of their mannose-6-phosphate (M6P) tag, on a N-linked glycan, to the extracellular domain of the cation-independent M6P receptor (29). Surprisingly, fibroblast uptake of recombinant human or mouse SGSH, produced in Chinese hamster ovary (CHO) cells, could only partially be blocked by 5 mM M6P, suggesting an additional uptake mechanism (30, 31). Furthermore, mutation of a N-glycosylation site (N264Q) in SGSH resulted in an enzyme unable to be blocked by M6P (32, 33). In addition to the M6P receptors, other receptors (*e.g.*, mannose receptor) have also been implicated in trafficking lysosomal enzymes independent of M6P binding (34). The identity of this additional sulfamidase trafficking receptor was unknown.

In this study, we generated fully active rhSGSH and identified LRP1 as the second SGSH uptake receptor in fibroblasts. We then evaluated the brain distribution, half-life, and durability of effect after a single dose. Based on that evaluation, we conducted a weekly 148 μg rhSGSH dosing study analyzing the brain for total HS, disease-specific HS-NRE, and protein biomarkers for disease pathogenesis. Lastly, we conducted a dose–response study and tested every other week dosing in a pilot experiment. Taken together, these data show that weekly 148 μg ICV doses, and perhaps less frequently, can lead to normalization of HS storage and reduction in disease biomarkers.

Results

rhSGSH utilizes two receptor-mediated mechanisms for cellular uptake in patient fibroblasts

Selected clones of CHO cells expressing recombinant human SGSH were generated. Harvest fluids from 14-day fed batch runs were purified using either a two-step (anion exchange and hydrophobic interaction chromatography) or a three-step (addition of ceramic hydroxyapatite type I) purification scheme. Purified enzyme was concentrated and buffer exchanged into artificial CSF suitable for injection. One lot from the two-step (Lot 1) and one lot from the three-step purification (Lot 2) were used in our studies. Prior to use, the enzyme was characterized for specific activity, percent F-gly conversion, purity, aggregation by size-exclusion chromatography (SEC), and N-glycan analysis.

As part of the characterization process, rhSGSH was evaluated for uptake into MPS IIIA patient fibroblasts at increasing concentrations for 4 h. Fibroblast uptake was only partially blocked by competition with 5 mM M6P (Fig. 1*A*). The M6P-dependent uptake contributed ∼60% at the lowest rhSGSH exposure (0.8 nM) and decreased to ∼20% as the rhSGSH concentration (51.8 nM) increased. These data agree with previous studies suggesting an additional lower affinity rhSGSH trafficking receptor (30–33) in fibroblasts. We set out to identify the additional receptor by competing with ligands to known alternative lysosomal enzyme trafficking receptors in the presence or absence of 5 mM M6P competition (34). Ligands for low-density lipoprotein receptor (LDLR), lysosomal integral membrane protein 2 (LIMP2), sortilin, as well as an antilysosomal associated membrane protein 2 (LAMP2) antibody were evaluated. Only alpha-2-macroglobulin receptor-associated protein (RAP) competed with rhSGSH for uptake at 50 nM (Fig. 1*A*). When rhSGSH was coincubated with 5 mM M6P and 50 nM RAP, all fibroblast uptake was blocked (Fig. 1*B*). RAP is a chaperone protein, but also blocks ligand binding, for the LDL receptor family (35). To confirm the identity of the second receptor, we evaluated mouse embryonic fibroblasts (MEFs) with either heterozygous or homozygous gene deficiency in low density lipoprotein-receptor related protein 1 (LRP1) for their ability to take up rhSGSH (36). LRP1-deficient cells had significantly reduced ability to endocytose rhSGSH (Fig. 1*C*). Combining LRP1 deficiency with 5 mM M6P competition blocked all rhSGSH uptake into MEFs (Fig. 1*D*). Thus, both LRP1 and CI-MPR mediate rhSGSH cellular uptake in fibroblasts.

ICV administration of rhSGSH results in widespread distribution of enzyme throughout the brain

Twelve-week-old MPS IIIA mice were implanted with a cannula in the left lateral ventricle of the brain and dosed with either vehicle (n = 6) or 148 μg of rhSGSH (Lot 1, n = 8) four times over 2 weeks. Twenty-four hours after the last dose, the contralateral side of the brain was harvested, formalin fixed and paraffin embedded, and sagittal sections were stained for rhSGSH by fluorescent immunohistochemistry (Fig. 2*A*). rhSGSH was detectable at the highest levels near the anterior cingulate area of the cortex but also, with various intensities, throughout the entire brain section as seen in the somatomotor areas of the cortex, striatum, thalamus, hypothalamus, and cerebellum (Fig. 2, *A* and *B*). rhSGSH staining of the cerebellar (Fig. 2*B*), ventral, and dorsal surfaces of the brain (Fig. 2*C*), which are not observed in the anti-hSGSH stained

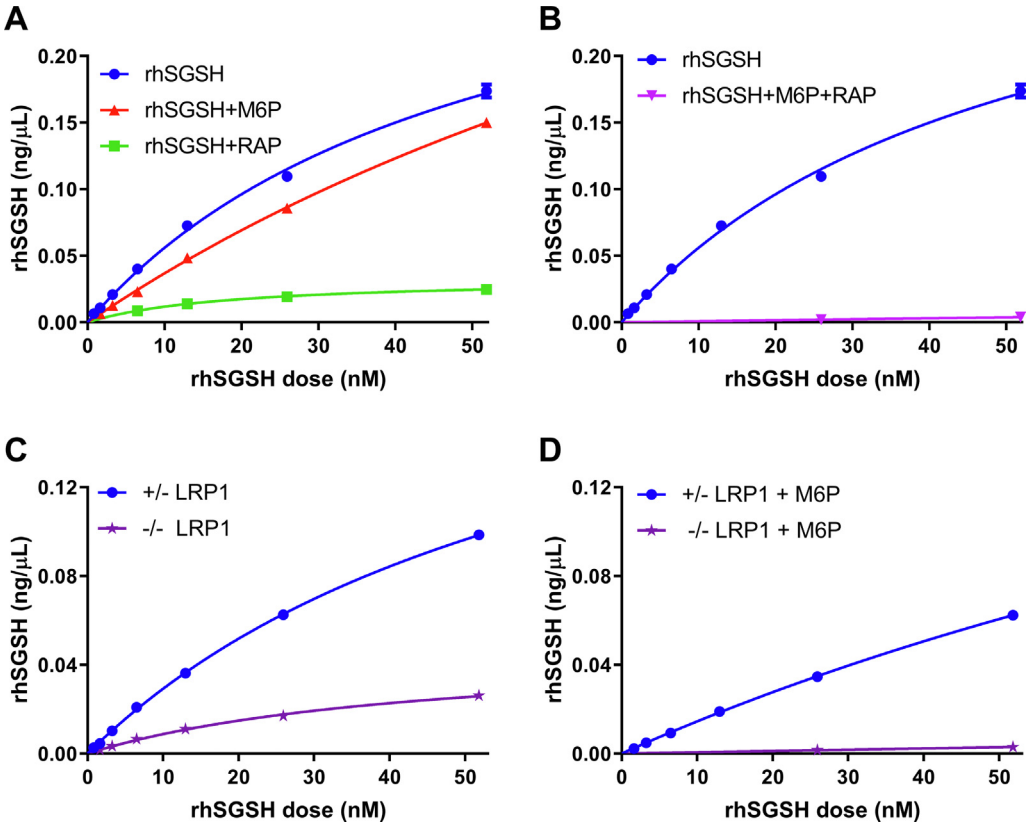

Figure 1. rhSGSH utilizes a two receptor-mediated mechanism for fibroblast uptake. *A*, uptake of rhSGSH in MPS IIIA patient fibroblasts is partially blocked by either 5 mM M6P or 50 nM RAP. *B*, the combination of 5 mM M6P and 50 nM RAP competition blocks all uptake. *C*, LRP1 is partially required for rhSGSH uptake in MEFs. *D*, 5 mM M6P competition reduces uptake in LRP1 heterozygous MEFs but completely blocks uptake in LRP1 deficient MEFs. MEF, mouse embryonic fibroblast; MPS, mucopolysaccharidosis; rhSGSH, recombinant human SGSH.

vehicle-treated MPS IIIA mice (Fig. 2*D*), suggesting a meningeal distribution of rhSGSH in addition to the brain parenchyma. Confocal fluorescent immunohistochemistry imaging from another experimental animal shows the partial rhSGSH colocalization with the lysosomal marker LAMP2 within the cortex (Fig. 2*E*).

A single high dose of rhSGSH dramatically reduces stored substrate in MPS IIIA mice

Following a single ICV administration of either vehicle (n = 4) or 161 μg of rhSGSH (Lot 2, n = 6) in 12-week-old MPS IIIA mice, brains were harvested and the tissue half-life and the durability of effect were determined to guide future experimental design. The dosed mice were sacrificed at 1 day post dose or at weekly intervals out to day 56 post dose or 20 weeks of age. The calculated brain tissue half-life was determined to be approximately 9.2 days (n = 6) (Fig. 3*A*). Using Sensi-Pro analysis, both total HS and the disease-specific HS-NRE rapidly declined within the first day and reached a nadir 2 weeks post dose (Fig. 3, *B* and *C*). WT animals were not originally included in this pharmacodynamic study; however, brain homogenates from the 19-week-old WT mice (n = 8), shown in Figure 4, were reassayed in this study for comparison and show that WT levels were not achieved after the single dose.

In addition to rhSGSH, a total of 51 proteins were analyzed from the brain homogenates over the time course by proteomics analysis using relative quantitation (Table S1). A selected subset is shown representing different aspects of the brain pathology (Fig. 3*D*). Lysosomal distention and quantity, and thus storage, is indirectly represented by the levels of the membrane protein lysosomal associated membrane protein 1 (LAMP1) and the soluble hydrolase Cathepsin B. We also selected three proteins, glial fibrillary acidic protein (GFAP), Progranulin, and complement C1q subcomponent C (C1QC), which have been reported to be elevated in neurodegenerative diseases as part of the neuroimmune response (38–41). The levels of these biomarkers in the vehicle-treated MPS IIIA mice (n = 2–4) were elevated, while levels in rhSGSH-treated MPS IIIA mice (n = 2–6) were significantly reduced (Fig. 3*D*). These reductions resulted in levels similar to WT (n = 4, remeasured WT samples from Fig. 4) with the treatment effect lasting up to 56 days post dose.

Weekly dosing of rhSGSH results in near normalization of brain HS storage, reduction in secondary lysosomal elevations, and reduction in selected neuroimmune response proteins

Given that total HS and HS-NRE both reached a nadir 2 weeks after a single dose (Fig. 3, *B* and *C*) and with rhSGSH having a brain tissue half-life of 9.2 days (Fig. 3*A*), we hypothesized that weekly dosing would lead to a further sustained reduction in lysosomal storage. Beginning at 12 weeks of age, MPS IIIA mice received eight weekly 148 μg doses of

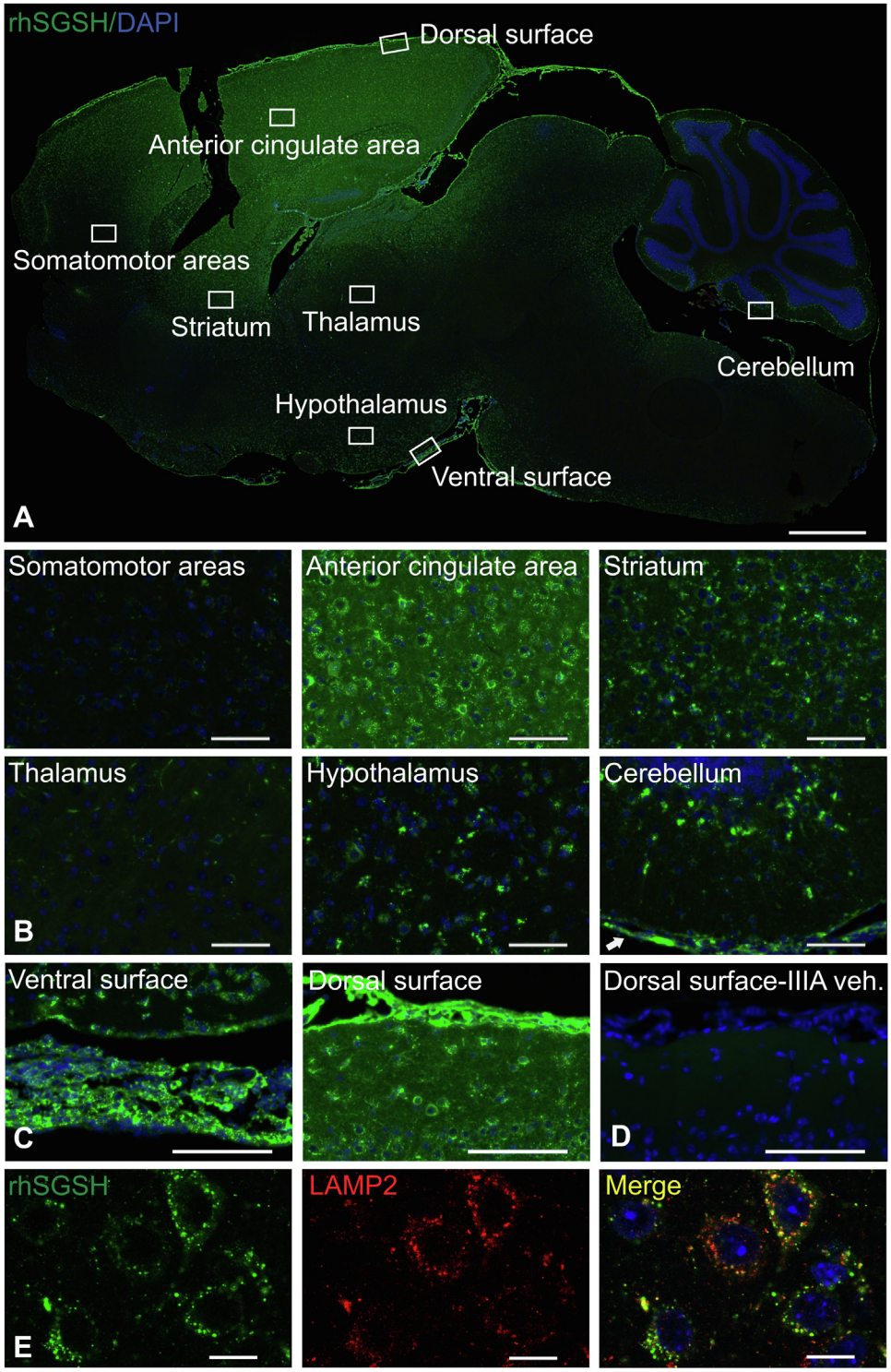

Figure 2. Intracerebroventricular administration of rhSGSH results in widespread distribution of enzyme throughout the brain. Beginning at 12 weeks of age, MPS IIIA mice received four 148 μg doses of rhSGSH or vehicle over 2 weeks and brains were processed 1 day after the last dose and stained with an anti-hSGSH antibody. A sagittal view (*A*) and insets (*B* and *C*) of a rhSGSH-treated MPS IIIA mouse. The *arrow* in the cerebellum inset highlights the staining of the meninges, which is also shown in the dorsal and ventral surface insets (*C*). *D*, a region-matched vehicle-treated MPS IIIA mouse stained with anti-hSGSH showing the rhSGSH dependency of the surface staining observed in (*C*). *E*, confocal images from a separate rhSGSH-treated animal costained for anti-hSGSH and anti-LAMP2 showing the degree of lysosomal colocalization. The scale bars represent (*A*) sagittal 1000 μm, (*B–D*) insets 50 μm, (*E*) confocal 10 μm. n = 2 of 8 rhSGSH-treated (one sagittal/insets and one confocal) and n = 1 of 6 vehicle-treated mice shown. MPS, mucopolysaccharidosis; rhSGSH, recombinant human SGSH.

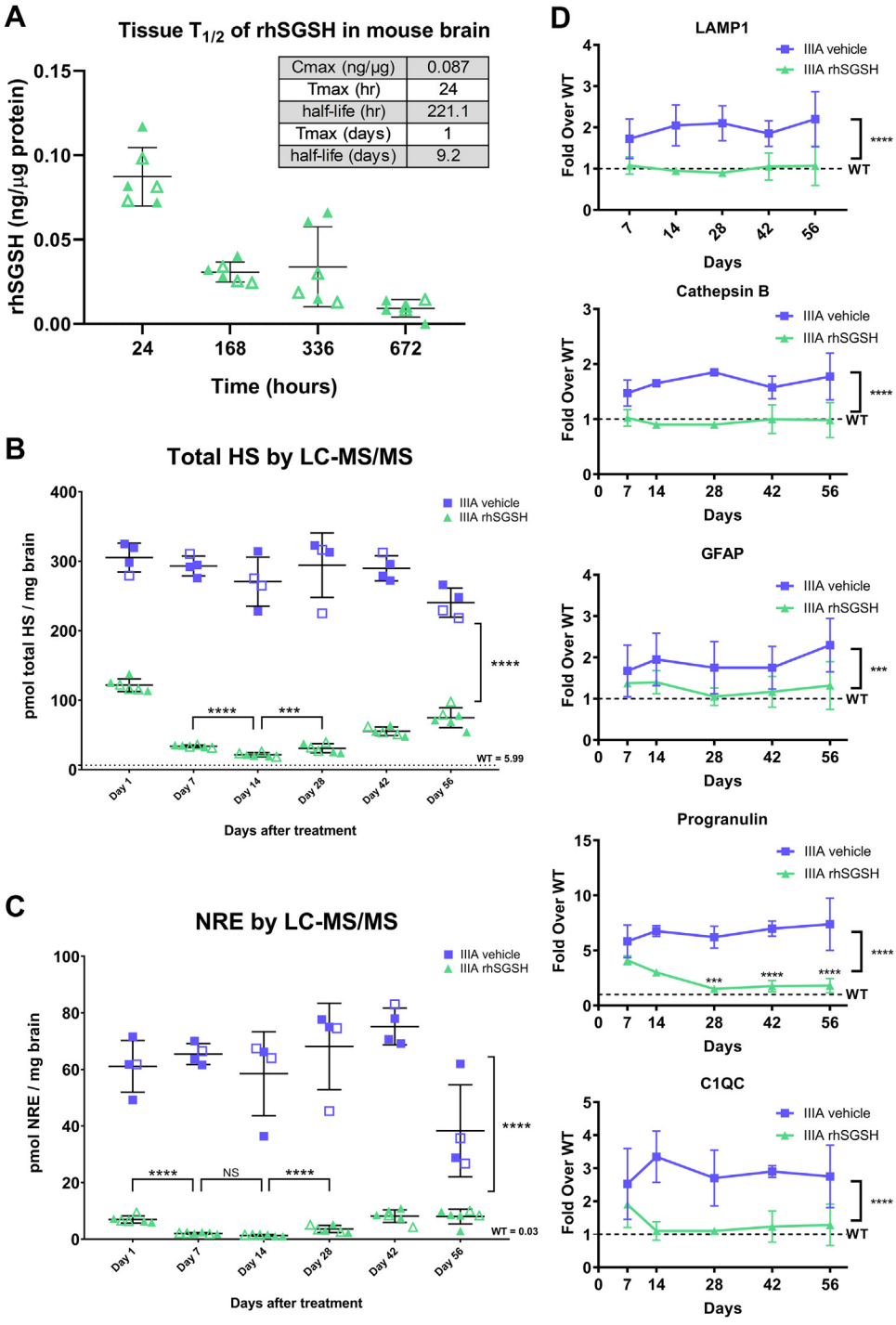

Figure 3. A single high dose of rhSGSH (161 µg) ICV dramatically reduces stored substrate in 12-week-old MPS IIIA mouse brain. *A*, rhSGSH half-life in brain tissue (n = 6). PK parameters determined with PKSolver (37). Sustained reduction over 56 days of (*B*) total heparan sulfate (HS), (*C*) total disease-specific HS-NRE, and (*D*) selected protein biomarkers (*B* and *C*: IIIA rhSGSH n = 6, IIIA vehicle n = 4; *D*: IIIA rhSGSH n = 2–6, IIIA vehicle n = 2–4). Relative quantitation of selected protein biomarkers (*A* and *D*) were determined by LC-PRM and absolute quantitation of total HS (*B*) and HS-NRE (*C*) were determined by LC-MS/MS with the WT samples (*B*, *C*: n = 8; *D*: n = 4) from Figure 4 being completely remeasured. Error bar = SD, NS = not significant, ***$p < 0.001$, ****$p < 0.0001$. *A–C*, open symbols are female mice and filled symbols are male mice. *D*, filled symbols are mixed gender. HS-NRE, heparan sulfate nonreducing end; ICV, intracerebroventricular; LC-PRM, liquid chromatography-parallel reaction monitoring; MPS, mucopolysaccharidosis; PK, pharmacokinetics; rhSGSH, recombinant human SGSH.

rhSGSH (Lot 1, n = 8) or vehicle (n = 8) and were compared to WT mice treated with vehicle (n = 8). Twenty-four hours after the last dose, brains were harvested, and the left hemisphere was analyzed for total HS and HS-NRE levels. Vehicle-treated MPS IIIA mice had mean total HS levels (288.11 ± 29.26 pmol/mg brain) that were 47.4-fold above WT (6.08 ± 0.83 pmol/mg brain; range: 5.00–7.17 pmol/mg brain) and mean HS-NRE levels (64.88 ± 6.21 pmol/mg brain) that were 648.8-fold above WT (0.10 ± 0.14 pmol/mg brain; range: 0.01–0.46 pmol/mg brain). Weekly rhSGSH treatment reduced mean

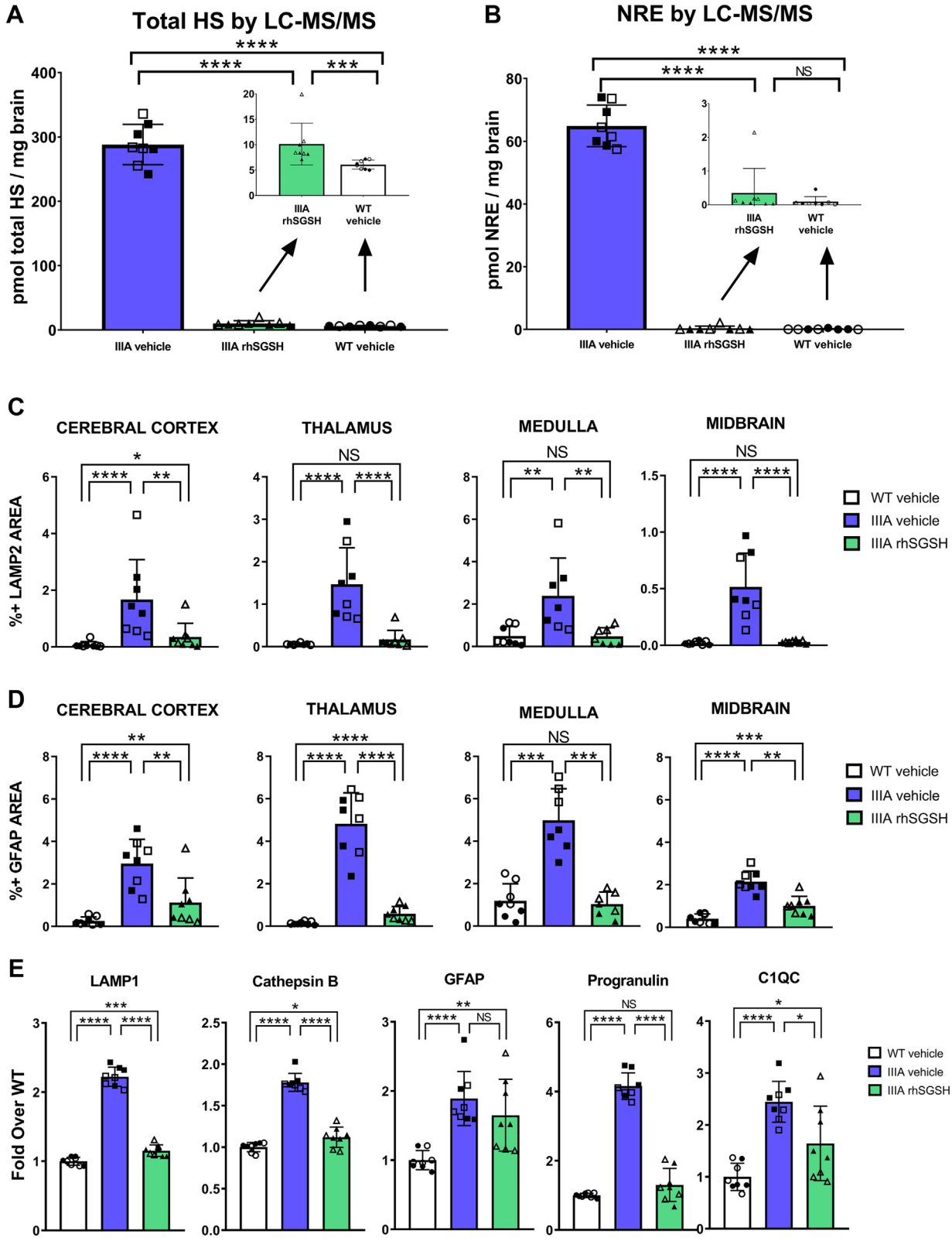

Figure 4. Eight weekly 148 µg doses of rhSGSH ICV, beginning at 12-weeks of age, result in normalization of brain-accumulated heparan sulfate (HS) storage and reduction in secondary lysosomal elevations and markers of a neuroimmune response. Brains were harvested 24 h after the last dose. Total HS (*A*) and HS-NRE (*B*) were measured by LC-MS/MS (n = 8). The levels of LAMP2 (*C*) and GFAP (*D*) by immunofluorescence staining in four brain regions (n = 7–8). *E*, relative quantitation performed by LC-PRM shows the levels of LAMP1, Cathepsin B, GFAP, Progranulin, and C1QC in total brain protein extract (n = 8). Error bar = SD, NS = not significant, *$p < 0.05$, **$p < 0.01$, ***$p < 0.001$, ****$p < 0.0001$. Open symbols are female mice and filled symbols are male mice. HS-NRE, heparan sulfate nonreducing end; ICV, intracerebroventricular; LC-PRM, liquid chromatography-parallel reaction monitoring; rhSGSH, recombinant human SGSH.

total HS by 96.5% (10.13 ± 3.85 pmol/mg brain; range: 7.13–19.93 pmol/mg brain) to 1.7-fold above WT (still significantly different from WT, $p < 0.001$) and mean HS-NRE by 99.5% (0.35 ± 0.68 pmol/mg brain; range: 0.03–2.15 pmol/mg brain) to 3.5-fold above WT (not different than WT, $p > 0.05$) (Fig. 4, *A* and *B*). Seven out of eight MPS IIIA animals treated with rhSGSH were in a narrow range of total HS (range: 7.13–10.70 pmol/mg brain) and the HS-NRE (range: 0.03–0.19 pmol/mg brain) was normalized to WT levels.

The distribution of the lysosomal and neuroimmune responses to substrate reduction were evaluated by measuring LAMP2 and GFAP levels, respectively, by immunofluorescence in sagittal sections of the right brain hemisphere. While globally affected, we quantified the LAMP2 staining in four specific locations (cerebral cortex [two areas], thalamus, medulla, and midbrain) within sagittal sections of the right brain hemisphere (Fig. 4*C*). In all four areas, the levels of LAMP2 staining in vehicle-treated MPS IIIA mice (n = 8) were significantly elevated compared to WT mice (n = 8). All four regions were significantly reduced in the rhSGSH-treated MPS IIIA mice (n = 8) compared to MPS IIIA mice treated with vehicle and were not significantly different than WT mice in three regions with the exception of the cerebral cortex (Fig. 4*C*). Within those same brain regions, we quantified the levels of GFAP staining (Fig. 4*D*). In all four areas, the levels of GFAP staining in vehicle-treated MPS IIIA mice were significantly elevated compared to WT mice. rhSGSH treatment resulted in a significant reduction in all four regions. While GFAP staining was reduced in all four regions of rhSGSH-treated mice, it was down to WT mice levels only in the medulla (Fig. 4*D*). Representative images of each group, brain region, and marker are shown in Figure S1.

Using the left brain hemisphere homogenates, relative levels of the previously selected lysosomal and neuroimmune response proteins were determined by the liquid chromatography-parallel reaction monitoring (LC-PRM) method (Fig. 4*E*, n = 8 per group). Both LAMP1 and Cathepsin B were significantly elevated in vehicle-treated MPS IIIA mice relative to the vehicle-treated WT counterparts and, although significantly different than WT, were nearly normalized with the weekly dosing. Progranulin and C1QC were significantly elevated in vehicle-treated MPS IIIA mice relative to vehicle-treated WT animals and significantly reduced upon treatment. While Progranulin levels were normalized with the treatment, the C1QC levels remained significantly elevated. In contrast to the immunofluorescent staining, the relative levels of GFAP measured by LC-PRM remained significantly elevated and virtually unchanged with treatment. Finally, serum levels of LAMP1, Cathepsin B, and Progranulin were measured by LC-PRM and compared to the brain levels (Fig. S2). Overall, the levels of these biomarkers correlated between the brain and serum ($R^2 > 0.5$). The rhSGSH-treated MPS IIIA samples clustered with the vehicle-treated WT samples, suggesting transfer between the compartments (brain/CSF and blood) of either CSF-derived rhSGSH and its biological effects or the biomarkers themselves.

A pilot study supports less than weekly dosing

The presence of rhSGSH and continued substrate clearance greater than 1 week after dosing suggested that every other week dosing may be efficacious (Fig. 3). Therefore, we conducted a pilot experiment to test this hypothesis by treating 12-week-old MPS IIIA mice with vehicle (n = 2) or 148 μg of rhSGSH (Lot 1, n = 2) every other week for four doses. The left brain hemispheres were harvested 1 week after the last dose and analyzed for total HS, HS-NRE, and the selected lysosomal and neuroimmune response biomarkers (Fig. 5). For the two rhSGSH-treated MPS IIIA mice, the levels of total HS were significantly reduced (19.81 and 5.33 pmol/mg brain) when compared to the two vehicle-treated MPS IIIA mice (267.78 and 207.71 pmol/mg brain) (Fig. 5*A*). The levels of HS-NRE were also significantly reduced in the two rhSGSH-treated MPS IIIA mice (0.55 and 0.17 pmol/mg brain) when compared to the two vehicle-treated MPS IIIA mice (58.97 and 17.68 pmol/mg brain) (Fig. 5*B*). In addition, we also compared by LC-PRM the brain levels of LAMP1, Cathepsin B, GFAP, Progranulin, and C1QC after rhSGSH or vehicle treatment in the MPS IIIA mice or with retested WT samples (n = 4) from Figure 4. LAMP1, Cathepsin B, Progranulin, and C1QC all showed an apparent reduction upon treatment (no difference amongst cohorts was seen with respect to GFAP). While a larger study is warranted to confirm these observations, it suggests that less frequent dosing may also lead to near normalization.

rhSGSH dose–response in mice suggests lower doses are feasible

In addition to the pilot experiment assessing the dose frequency needed to achieve normalization, we also evaluated the dose. Twelve-week-old MPS IIIA mice (n = 7 per group) were treated with a single 36 μg, 77.5 μg, 161 μg, or 293.5 μg ICV dose (all derived from Lot 2), and 2 weeks post dose, the left brain hemisphere of each animal was analyzed for rhSGSH, total HS, HS-NRE, and the selected lysosomal and neuroimmune response biomarkers (Fig. 6). rhSGSH levels were measured by LC-PRM and showed a dose-dependent increase with increasing dose (Fig. 6*A*). Total HS was significantly reduced by 86.4% for the 36 μg dose, 91.5% for the 77.5 μg dose, 93.7% for the 161 μg dose, and 94.2% for the 293.5 μg dose relative to the vehicle-treated MPS IIIA mice (Fig. 6*B*). The total HS levels with the 36 μg dose was significantly higher than all other doses. The 77.5 μg dose led to significantly lower HS levels than the 36 μg dose, was not significantly different than the 161 μg dose, but remained significantly elevated compared to the 293.5 μg dose. The total HS levels were not significantly different between the 161 μg and 293.5 μg doses. HS-NRE was significantly reduced by 91.4% for the 36 μg dose, 96.5% for the 77.5 μg dose, 98.5% for the 161 μg dose, and 99.0% for the 293.5 μg dose relative to the vehicle-treated MPS IIIA mice (Fig. 6*C*). HS-NRE level with the 36 μg dose was significantly elevated than all other doses. The 77.5 μg dose led to significantly lower HS-NRE levels than the 36 μg dose but remained significantly elevated compared to both the 161 μg

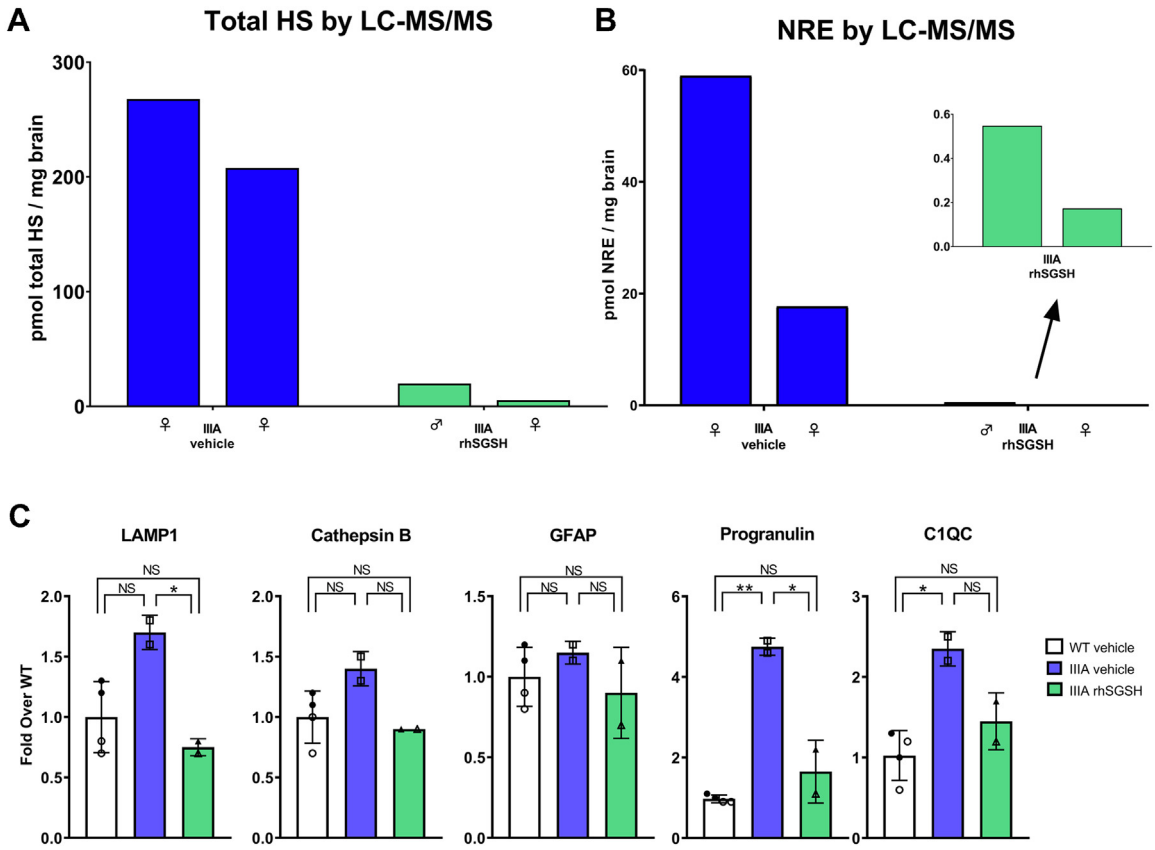

Figure 5. A pilot, every other week dosing study suggests less frequent dosing is feasible. Beginning at 12 weeks of age, two MPS IIIA mice received rhSGSH (148 μg) and two MPS IIIA mice received vehicle every other week for 7 weeks (4 total doses). Brains were harvested 7 days after the last dose to mirror the takedown age in Figure 4. Absolute brain levels of total HS (*A*) and total HS-NRE (*B*) were determined by LC-MS/MS. *C*, relative quantitation performed by LC-PRM shows the levels of LAMP1, Cathepsin B, Progranulin, C1QC, and GFAP in total brain protein extract. *C*, WT samples (n = 4) from Figure 4 were reanalyzed with these samples. Error bar = SD, NS = not significant, $*p < 0.05$, $**p < 0.01$. *A* and *B*, columns are labeled with gender. *C*, open symbols are female mice and filled symbols are male mice. HS-NRE, heparan sulfate nonreducing end; LC-PRM, liquid chromatography-parallel reaction monitoring; MPS, mucopolysaccharidosis; rhSGSH, recombinant human SGSH.

and 293.5 μg doses. The HS-NRE levels were not significantly different between the 161 μg and 293.5 μg doses. Lastly, we analyzed the brain levels of LAMP1, Cathepsin B, GFAP, Progranulin, and C1QC in the rhSGSH-treated MPS IIIA mice compared to the vehicle-treated MPS IIIA mice at the different dose levels (Fig. 6*D*). The levels of LAMP1, Cathepsin B, Progranulin, and C1QC were significantly reduced relative to vehicle-treated MPS IIIA mice at all dose levels. For GFAP, only the 161 μg and 293.5 μg doses were significantly reduced relative to the vehicle-treated MPS IIIA mice. The differences between dose levels of LAMP1, Cathepsin B, GFAP, Progranulin, and C1QC were not significant.

Discussion

In this study, we generated CHO-produced fully active rhSGSH and characterized its uptake into MPS IIIA patient fibroblasts. The identity of the M6P-independant uptake receptor in fibroblasts was identified as LRP1. In juvenile (P5) and adult (P60) mouse brains, LRP1 is expressed in microglia, astrocytes, and neurons but not in oligodendrocytes nor parvalbumin-positive interneurons (42). The mechanism by which rhSGSH interacts with LRP1 is unknown. RAP's interactions with LRP1 are thought to be mediated by lysines on the surface of RAP (43). Surprisingly, recent data on CHO produced rhSGSH treated with sodium metaperiodate and sodium borohydride, to chemically alter the carbohydrates and thus reduce carbohydrate-dependent cellular uptake, resulted in a nearly complete reduction in uptake into an MPS IIIA patient fibroblast line (23). These data suggest that the interaction of rhSGSH with LRP1 might be mediated, at least in part, by a carbohydrate moiety on rhSGSH instead of lysine. Regardless, the ability to interact with both CI-MPR and LRP1 may facilitate a more rapid or widespread uptake into cells of the brain. Lastly, the potential for rhSGSH to compete with endogenous LRP1 ligands might favor an intermittent ERT approach over therapeutics that continuously deliver or secrete enzyme (44).

HS is a component of the cellular glycocalyx. When it is endocytosed and reaches the lysosome, it is cleaved by the endoglycosidase heparanase (HPSE) between glucuronic acid and N-sulfoglucosamine residues (45). Subsequently, the resulting HS fragments are degraded in a stepwise manner from the nonreducing end by a series of exoglycosidases and exosulfatases as well as the N-acetyltransferase HGSNAT (46). Heparanase generates multiple fragments from each HS molecule that enters the lysosome, increasing the number of HS-NREs for the lysosomal system to process. In MPS IIIA,

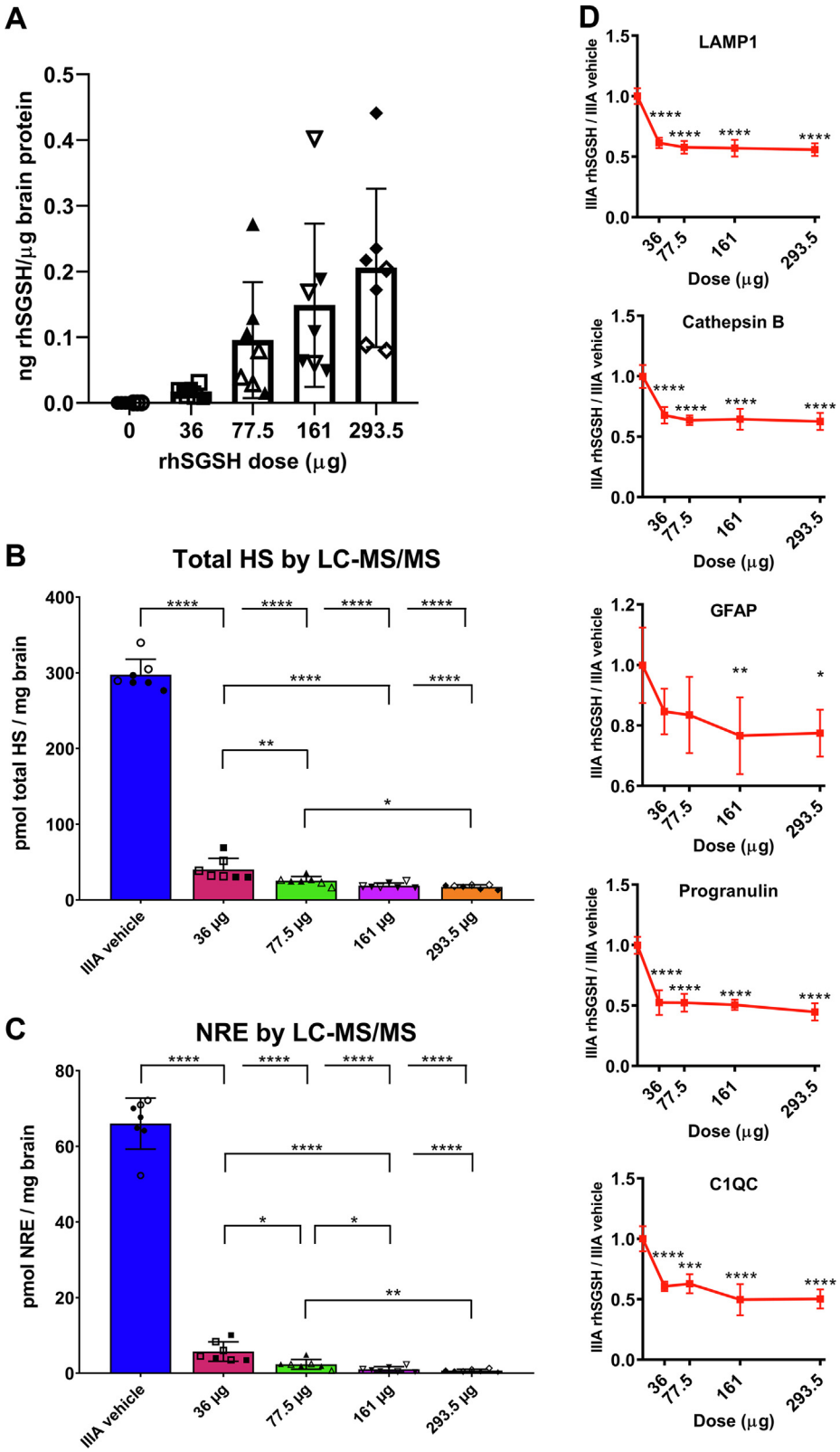

Figure 6. A single rhSGSH dose–response in brain analyzed at 14 days post dose (n = 7). The age at dosing was 12 weeks. Increasing dose leads to higher rhSGSH brain levels (*A*). Multiple doses significantly reduced total heparan sulfate (*B*), disease-specific HS-NRE (*C*), and selected biomarkers (*D*). Error bar = SD, *$p < 0.05$, **$p < 0.01$, ***$p < 0.001$, ****$p < 0.0001$. *A–C*, open symbols are female mice and filled symbols are male mice. *D*, filled symbols are mixed gender. HS-NRE, heparan sulfate nonreducing end; rhSGSH, recombinant human SGSH.

these HS fragments are degraded until N-sulfoglucosamine, the substrate for SGSH, is revealed; SGSH deficiency blocks further degradation. As a result, HS fragments with the MPS IIIA-specific N-sulfoglucosamine HS-NRE moiety accumulate and are a direct measure of the substrate of SGSH while total HS is a measure of the associated HS polymer. Thus, restoring SGSH activity to MPS IIIA patients is the most direct therapeutic approach to this disease.

A natural history study has shown that CSF HS levels in MPS IIIA patients can range from approximately 2 to 10 μM, nearly an order of magnitude (47). Thus, a treatment that reduced CSF HS levels in a patient from 10 μM to 2 μM, an 80% decrease, would still result in a level of HS consistent with other MPS IIIA patients. A more appropriate goal for SGSH replacement therapies should be to reduce CSF HS and HS-NRE into the normal range to obtain the maximal potential clinical benefit. As shown in Figure 4*B*, weekly dosing of 148 μg rhSGSH did indeed reduce the disease-specific HS-NRE in seven of the eight MPS IIIA animals (range: 0.03–0.19 pmol/mg brain for the seven mice) into the WT range (0.01–0.46 pmol/mg brain). However, the mean total HS for the same seven rhSGSH-treated mice (range: 7.13–10.70 pmol/mg brain) remained just above the tested WT range (range: 5.00–7.17 pmol/mg brain).

Our studies illustrate why it is critical to use state-of-the-art LC-MS technologies that have sufficient sensitivity to measure HS in unaffected samples in preclinical and clinical MPS III studies. There are several assays that are currently used to measure HS, each with their own characteristics and sensitivities (25). The ability to quantify normal levels of HS and HS-NRE in tissues and CSF is critical to bridge preclinical and clinical studies in evaluating the biochemical restoration of lysosomal function. To that end, in both MPS IIIA and MPS II mice, brain HS levels were shown to correlate with CSF HS levels, and in the case of MPS IIIA, the correlation remained even with different amounts of HS reduction by recombinant enzyme treatment (23, 48). These data support using quantification of HS and HS-NRE in the CSF as a surrogate for brain accumulation. However, without the ability to quantify normal levels of HS or HS-NRE in CSF, it is impossible to know if the therapeutic response is bringing patients into the normal range or only partially reducing the substrate burden. For example, using the methods hereby presented, total HS was elevated 47.4-fold and HS-NRE 648.8-fold in the brains of MPS IIIA mice as compared to WT ones (Fig. 4, *A* and *B*). A hypothetical 75% reduction in those amounts would still result in levels of HS and HS-NRE that are 11.9-fold and 162.2-fold above normal, respectively. While a 75% reduction might look significant, it is unlikely to be sufficient to restore lysosomal function within a normal range and consequently achieve therapeutic benefit. Furthermore, a direct correspondence between changes in CSF HS/HS-NRE levels and the worsening or amelioration of clinical disease has not been established. While normalizing biochemical function is likely a prerequisite, additional factors are expected to contribute to the best clinical outcomes, such as the patient's age and degree of brain atrophy at treatment onset, the duration of treatment, and the fraction of the delivered dose taken up by the brain *versus* CSF drainage to the periphery. Earlier treatment in MPS VII mice has previously been shown to be more efficacious than delayed treatment (49).

In a phase I/II study in MPS IIIA patients, six monthly intrathecal doses of rhSGSH (10 mg, 45 mg, or 90 mg) reduced CSF HS, with the 90 mg cohort showing a 58% to 75% decline from baseline (26). For the 48-week phase IIb clinical trial, a 45 mg dose of rhSGSH was delivered intrathecally every other week or monthly (27). While a considerable reduction in CSF HS was observed in both cohorts, the treatment failed to consistently bring HS in the CSF to normal levels. The partial restoration of lysosomal HS degradation left substrate levels within the disease range and the study failed to achieve its primary end point. These data imply that normalization is a prerequisite for efficacy and suggest that the age at treatment initiation is important, that is, the earlier the better.

In our current preclinical studies, a 148 μg dose (approximately equivalent to a 296 mg human equivalent dose [h.e.d.]) delivered weekly ICV in MPS IIIA mice normalized the disease-specific HS-NRE in seven out of eight mice. In addition, similar effects on total HS and HS-NRE levels were seen after a single administration of either 161 μg (322 mg h.e.d.) or 293.5 μg (587 mg h.e.d.) of rhSGSH, suggesting a plateaued effect. However, less reduction in HS and HS-NRE were observed in animals administered with either a 77.5 μg (155 mg h.e.d.) or 36 μg (72 mg h.e.d.) dose of recombinant enzyme. The partial reduction in brain substrate levels observed with the lower doses is similar to the CSF data reported in the human MPS IIIA trials (26, 27). In our study, both total HS and HS-NRE reached a nadir 14 days after a single administration of 161 μg of rhSGSH; HS and HS-NRE levels started to rebound by day 28. For both, total HS and HS-NRE, brain levels on day 28 were significantly higher than on day 14 (1.4-fold, $p < 0.001$ and 2.7-fold $p < 0.0001$, respectively), suggesting a monthly dose of 161 μg might be insufficient. These preclinical data imply that higher doses and/or dosing frequencies, than previously tested in the clinic, should bring CSF HS in MPS IIIA patients into the normal range, a prerequisite to clinical efficacy.

Published data in MPS IIIA mice and dogs suggests the process and route of administration may also affect the efficacy of an ERT approach. A MPS IIIA dog study compared intrathecal lumbar, intrathecal cisterna magna, and ICV administration of a 3 mg dose (four weekly followed by four every other week, 30 mg h.e.d.). While the three routes of treatment showed similar responses in HS (brain and CSF) and secondary markers throughout the brain, the ICV route approached normalization of the activated microglia marker in both the superficial and deep cortex (12). Beard *et al.* compared the effect of a single dose of 100 μg of rhSGSH (200 mg h.e.d.) given in mice ICV (split equally and injected into each of the two lateral ventricles), intrathecally in a cisterna magna injection or through a lumbar injection. One week post dosing, a hemicoronal brain slice containing the cerebellum and brain stem was analyzed for total HS. The ICV dosing resulted in the lowest HS levels (9). A 2-week mouse

study compared a weekly bolus dose of 100 μg of rhSGSH delivered intrathecally (cisterna magna) with ICV delivery by osmotic pump (over the course of the week), with the ICV/pump appearing to be more efficacious (10). Lastly, a study in the canine model used intrathecal administration to compare bolus and pump-based continuous dosing, with the bolus seemingly more efficacious (14). Taken together, the published studies suggest that bolus delivery of rhSGSH into the cisterna magna may yield less brain parenchymal enzyme uptake and distribution than ICV resulting in suboptimal HS/HS-NRE clearance (50).

A brain half-life of 9.2 days after a single 161 μg ICV rhSGSH administration (Fig. 3*A*) is consistent with data from others regarding *in vivo* lysosomal enzyme half-lives following ERT (51, 52). Such a half-life combined with a 2-week nadir in HS and HS-NRE levels (Fig. 3, *B* and *C*) potentially support weekly or every other week dosing in a clinical setting. Significant reaccumulation of HS and HS-NRE by day 28 post dose suggests inadequate rhSGSH activity by then. In a series of studies in MPS IIIA mice, Hemsley *et al.* evaluated intrathecal cisterna magna injections of rhSGSH at increasing dose levels every other week from 6 to 18 weeks of age (6–8). With increasing dose levels from 5 μg up to 100 μg (10–-200 mg h.e.d.), these studies observed improved reduction (up to 85%) of accumulated substrate (as measured by glucosamine-N-sulfate hexuronic acid, GlcNS-UA) across the brain and spinal cord. Consistent with these observations, we were able to achieve near normalization of HS and the MPS IIIA-specific HS-NRE with weekly 148 μg dosing ICV (296 mg h.e.d.). Our pilot study suggests that every other week administration might be sufficient to sustain the same effect (Fig. 5). The single dose–response study highlighted the possibility that a 77.5 μg dose (155 mg h.e.d.) might be as equally efficacious as a 161 μg dose (322 mg h.e.d.). Additional studies could evaluate these hypotheses and may help define the optimal dose and treatment regimen.

The similarity of the biochemical findings presented here in the MPS IIIA model to those previously reported in MPS IIIB are striking (28, 51). In both cases, it was found that the ICV delivery of a high dose of a deficient lysosomal enzyme was capable of eliminating the accumulated substrate. In the case of MPS IIIB, elimination of the disease-specific HS-NRE and normalization of total HS observed in the mouse model was effectively translated, with very similar effect, in a canine model (53). More importantly, normalization of total HS observed in both animal models effectively translated into HS normalization in MPS IIIB patients (54, 55). The critical implication from our current study is that ICV delivery of a sufficient amount of rhSGSH, higher than previously tested in humans, should be expected to eliminate substrate accumulation in MPS IIIA patients. Sustained CSF HS normalization is a likely prerequisite to clinical benefits.

In conclusion, higher doses of rhSGSH delivered ICV weekly normalized the MPS IIIA-specific HS-NRE and led to the reduction in brain and serum biomarkers. The conserved biochemistry between mouse and human allows for the biochemical evaluation of therapeutics as well as identification of potential translatable biomarkers (Fig. S2). However, the observation that reaccumulation of HS and HS-NRE preceded an increase in the lysosomal proteins LAMP1 and Cathepsin B highlight the importance of directly monitoring CSF HS and HS-NRE for dosing determinations. One aspect not evaluated in our studies is the possibility that earlier treatment may lead to better outcomes, as seen in MPS VII mice (49); however, testing this hypothesis is challenging in the mild MPS IIIA mouse model (56, 57). Taken together, our results support further clinical assessment of higher doses of rhSGSH delivered ICV for the treatment of MPS IIIA.

Experimental procedures

Cell culture

Recombinant human SGSH was expressed using the GS Gene Expression System (Lonza). CHO clones expressing rhSGSH (pXC-17.4, Lonza) and rhSUMF1 (pD2529, ATUM) were generated by MaxCyte electroporation (MaxCyte, Inc) and selected using the selectable markers. The clones with the highest expression and activity were identified and scaled up. Selected clones were run in a fed-batch process at 10L scale with CHO CD Efficient Feed B (ThermoFisher) added during the run along with proprietary additives. The bioreactors (10L BioFlo 320, Eppendorf or 10L Applikon, Applikon Biotechnology) were monitored for viable cell density, dissolved oxygen, pH, glucose, lactate, glutamine, and glutamate. Glucose was maintained above 2 g/l and the pH was set at 7, controlled using 0.5 M Na_2CO_3 and a CO_2 control loop. After a 14-day run, cell culture fluid was clarified by depth filtration (3M) and stored at −80 °C.

Purification

rhSGSH was purified from cell culture fluid using either a two or three step purification using an ÄKTA avant (GE Healthcare). Filtered harvest was diluted at a 1:2 volume ratio with 20 mM Tris, pH 7.3 and loaded onto a Capto Q ion exchange resin (GE Healthcare) and eluted with 250 mM NaCl. The Capto Q eluate was then adjusted to 20 mM Tris, 1 M ammonium sulfate, pH 7.3, and loaded onto a Capto Butyl hydrophobic interaction chromatography resin (GE Healthcare). Elution was generated by a linear gradient of declining ammonium sulfate. For purifications with three steps, the Capto Butyl eluate was diluted 6-fold with 2 mM phosphate, 20 mM Tris, pH 6.2, and loaded onto a ceramic hydroxyapatite type I resin (Bio-Rad Laboratories). Elution was achieved with a 50 mM phosphate, 20 mM Tris, 150 mM NaCl, pH 7.5 buffer. rhSGSH was formulated into artificial CSF (3 mM KCl, 5 mM phosphate, 150 mM NaCl, pH 7.3) and concentrated to 29.6 mg/ml for the two-step Lot 1 and 32.2 mg/ml for the three-step Lot 2 by ultrafiltration/diafiltration using a 30 kDa molecular weight cutoff polyethersulfone membrane. All lots were greater than 95% pure (RP-HPLC, Agilent C3 Zorbax 300SB) and within an endotoxin specification of ≤0.05 EU/mg rhSGSH (Endosafe PTS) whether the two-step or three-step purification was used.

Treatment of MPS IIIA with ICV delivery of rhSGSH

Characterization

ELISA

rhSGSH was quantified in cell culture fluid, during purification, and in cell lysates by ELISA (capture, H00006448-D01P Abnova; detection, ab72617 Abcam).

Enzyme activity

Activity was determined using a two-step method, wherein rhSGSH desulfated 4-MUGlcNS (EM06602, Carbosynth) followed by cleavage with alpha-glucosidase (G3651, Sigma) liberating 4-methylumbelliferone. The specific activity of Lot 1 was 65.0 pmol of 4-methylumbelliferone per ng of rhSGSH per hour (pmol/ng/hr) *versus* 67.8 pmol/ng/hr for Lot 2.

Fibroblast uptake

For uptake studies, MPS IIIA patient fibroblasts (GM00643, Coriell) and MEFs heterozygous (CRL-2216, ATCC) or null (CRL-2215, ATCC) for LRP1 were plated at a density of 2e5 cells per well. One day later, the cells were exposed for 4 h to different concentrations of rhSGSH with or without competition from 5 mM M6P (M6876, Sigma) and/or 50 nM RAP (4296-LR, R&D). Cells were washed three times with Hank's balanced salt solution, two times with PBS, and lysed in M-Per (78501, Thermo) with protease inhibitor (P8340, Sigma).

Formylglycine

To measure the level of formylglycine conversion, samples were labeled with 2-aminobenzamide and analyzed by reverse phase HPLC using a 100 min linear gradient of 15% to 100% mobile phase B (80% acetonitrile/0.05% TFA) mixed with mobile phase A (0.05% TFA). The integrated peak area of the fluorescent label (Ex: 330 nm, Em: 420 nm) was calculated relative to the integrated peak area for protein absorbance at 214 nm. A recombinant human arylsulfatase B with 100 percent conversion served as a reference comparator to calculate the percent conversion.

SEC

For SEC, the samples were diluted to 1 mg/ml with 2× DPBS and 10 μg injected onto a Zenix-C SEC-300 column (3 μm, 300 Å, 7.8 × 300 mm with 50 mm guard column, Sepax Technologies) set at 30 °C with a 2× DPBS mobile phase and a 0.5 ml/min flow rate on a 1100/1200 HPLC system (Agilent Technologies). The data were processed using the Agilent Chemstation software and compared to SEC molecular weight standards (Bio-Rad Laboratories).

N-glycan and CI-MPR binding analysis

N-linked glycosylation was determined essentially as previously described (51, 58). For binding analysis, CI-MPR was biotinylated (10:1 biotin to CI-MPR ratio), loaded onto a streptavidin-coated biosensor (at 10 μg/ml), and the binding affinity of rhSGSH was determined by performing a global fit of the association and dissociation curves at different rhSGSH concentrations on the Octet instrument (ForteBio).

Protein purity

For purity analysis, 5 μg of sample was injected onto a C3 Zorbax 300SB column (2.1 × 150 mm, Agilent Technologies) set at 45 °C with a 0.75 ml/min flow rate on a HPLC with a UV detector (Agilent Technologies). Samples were analyzed using mobile phase A (0.1% TFA in water) and mobile phase B (0.1% TFA in acetonitrile) in a gradient of 15% B for 3 min, 15% to 80% B for 32 min, hold 80% B for 5 min, and 80% to 15% B for 2 min. Data were processed using the Agilent Chemstation software.

Animal model, husbandry, and ICV injections

All studies were approved by the BioMarin Animal Resource Committee and the Institutional Animal Care and Use Committee of the Buck Institute for Research on Aging. SGSH-deficient mice (B6.Cg-Sgsh^{mps3a}/PstJ, Jackson Laboratory #003780) were maintained as a colony at the Jackson Laboratory and study mice maintained at the Buck Institute vivarium (59). Study animals were enrolled based on age, mixed gender, and with the intent of equal distribution of gender whenever possible. Study mice were fed food and water ad libitum and maintained on a 12 h light/dark cycle. Five days before first dosing, mice underwent surgery to implant the cannula under isoflurane anesthesia. The cannula was placed into the left lateral ventricle, cemented in place to the skull, and covered with a dummy cap. The skin was sutured together along with tissue glue. For each injection, the dummy cap was removed, the injector needle was connected, and 5 μl of vehicle or rhSGSH was infused by pump over the course of 15 min. Since a fixed volume of 5 μl was used, minor dose variation occurred depending on the Lot administered. *Ex vivo* sample analyses were conducted in an unblinded fashion.

Fluorescent immunohistochemistry

Twelve-week-old MPS IIIA mice received four 148 μg doses over a 2 week period into the left lateral ventricle. Twenty-four hours after the last dose, the right brain hemisphere (contralateral side) was harvested and fixed in formalin. The formalin-fixed paraffin-embedded brains were then sectioned at 5 μm and collected on Superfrost plus slides. Slides were stained using a Ventana Discovery Ultra autostainer (Ventana, Roche) using the following specifications. Antigen retrieval was performed at 95 °C for 32 min using Ventana Discovery CC1 antigen retrieval solution (950–500, Ventana). Sections were blocked in 2% normal donkey serum, 0.1% bovine serum albumin, and 0.3% Triton in 1× Tris-buffered saline for 1 h and then incubated with primary antibody followed by a fluorescent secondary antibody, both for 1 h at room temperature. Antibody specifications are as follows: LAMP2 (ab25339, Abcam) at 1:100 followed by a donkey antirat 488 (A21208, Life technologies) at 1:125 dilution. GFAP (G9269, Sigma) at 1:2000 followed by a donkey anti-rabbit 555 (A31572, Life technologies) at 1:125 dilution. SGSH (ab200346, Abcam) at 1:200 followed by a donkey anti-rabbit 488 (A21206, Life technologies) at 1:125 dilution. Nuclei were stained by 4′,6-diamidino-2-phenylindole. Slides were imaged on a Zeiss

Axio Scan.Z1 using a Plan-Apochromat 20×/0.8 objective equipped with a Hamamatsu Orca Flash camera. rhSGSH brain biodistribution was qualitatively assessed from full slice scans. Areas of select brain regions were extracted from the full slice scans and LAMP2 and GFAP stain were quantified. Regions were level adjusted in Photoshop and the percent area of stain was calculated using custom macros in ImageJ Fiji software (https://fiji.sc/) (60). Images depicting rhSGSH/LAMP2 colocalization were acquired on a Leica SP8 confocal microscope using a Plan Apo 63 × .1.4 objective with 2.5× zoom and pinhole set to 1AU.

Tissue homogenization

After perfusion, brains were isolated, halved into hemispheres, and the left hemisphere flash frozen in liquid nitrogen. Frozen samples were then homogenized in tubes preloaded with zirconium oxide beads (REDE-RNA, Next Advance) and 0.8 ml of cold HPLC grade water (Sigma) was added to each sample. Samples were homogenized three times with a Bullet Blender (Next Advance) for 3 min at speed 8 in a cold room (4 °C) with a resting period of 5 min between homogenization steps. An aliquot of this water brain homogenate was used for HS and HS-NRE analysis and another aliquot was mixed with 4 parts of lysis buffer (Biognosys) for proteomics analysis. The protein concentration of all samples was determined using a bicinchoninic acid assay (Thermo Fisher Scientific).

Proteomics sample preparation

Proteins were reduced and alkylated using Biognosys' reduction and alkylation buffers and digested overnight (70 μg protein/sample) with sequencing grade modified trypsin (Promega) at a protein:protease ratio of 50:1. C18 clean-up for mass spectrometry (MS) was carried out on a C18 96-well Micro Spin plate (The Nest Group) according to the manufacturer's instructions. Peptides were dried down to complete dryness using a Speed Vac system and redissolved in LC solvent A (1% acetonitrile in water with 0.1% formic acid [FA]) containing iRT-peptide mix (Biognosys) for retention time calibration. Peptide concentration was measured using a bicinchoninic acid assay kit (ThermoFisher). Six stable isotope-labeled reference peptides were spiked into the final peptide samples at known concentrations (JPT, the quality grade of the reference peptides was Maxi_Spike_Tides_QL_AAA [±10% quantification precision, >95% purity]).

Protein MS and proteomics

The amount of rhSGSH protein in MPS IIIA mouse brain protein extract was determined using LC-PRM–based targeted MS. Peptides (1 μg per sample) were injected onto an in-house packed C18 column (ReproSil-Pur120C18AQ, 1.9 μm, 120 Å pore size; 75 μm inner diameter, 50 cm length, New Objective) on a Thermo Scientific Easy nLC 1200 nano-LC system. Solvent A was 1% acetonitrile in water with 0.1% FA. Solvent B was 15% water in acetonitrile with 0.1% FA. The LC gradient was 5% to 40% solvent B over 60 min, ramped to 100% B over 2 min, and held at 100% B for 12 min (total gradient length was 75 min). rhSGSH pharmacokinetics was determined using PKSolver (37).

LC-PRM runs for peptide quantification were carried out on a Thermo Scientific Q Exactive mass spectrometer equipped with a standard nano electrospray source. Collision energies were 25 eV according to the vendor's specifications. The acquisition window was 6 min. A run in PRM mode was performed before data acquisition for retention time calibration using Biognosys' iRT concept (61). Signal processing and data analysis were carried out using SpectroDive 7.0 (Biognosys, based on mProphet) (62). A Q-value filter of 1% was applied. The absolute quantification was determined by comparing the abundance of the known internal standard peptides with the endogenous peptides. The ratio of the areas under the curve (between the endogenous and reference peptide) was used to determine the absolute levels of rhSGSH enzyme in the samples. The peptides used for absolute and relative quantification of rhSGSH are listed in Table S2. Samples for mass spectrometry ID discovery proteomics were prepared and run as recommended by Biognosys. A total of 51 proteins (Table S1) consisting of lysosomal and nonlysosomal proteins were analyzed using relative quantitation. These proteins were previously identified in an exploratory proteomics study as potential biomarkers in MPS IIIA mice. Three proteins were included as controls for sample preparation and loading (P16858 [G3P_mouse], P56480 [ATPB_mouse], P63260 [ATCT_mouse]). Four parts of Biognosys lysis buffer was added to one part of brain water homogenate. Protein intensities were analyzed in GraphPad Prism (GraphPad Software) and discoveries determined using the two-stage linear step-up procedure of Benjamini, Krieger and Yekutieli, with Q = 5%.

Sensi-Pro analysis

HS from mouse brain homogenate was purified, digested, and labeled with aniline as previously described (63). Briefly, glycosaminoglycans were purified by anion-exchange chromatography and subsequently enzymatically depolymerized into constituent HS-NRE and internal disaccharides with heparan lyases. Digestion products were then labeled by reductive amination with [$^{12}C_6$]-aniline before quantitative compositional analysis using LC-MS/MS. After labeling, digested HS samples were mixed with 40 pmoles of [$^{13}C_6$]-aniline labeled HS-NRE (*N*-sulfated glucosamine, S0) and internal disaccharide standards as previously described (25, 64). The sample and standard mixture was then dried down in a vacuum concentrator and reconstituted in 80/20 acetonitrile/water (v/v). Samples were then analyzed for 12 HS internal disaccharides and the MPS IIIA-related HS-NRE S0 with an Acquity UPLC attached to a Xevo TQ-S micro Triple Quadrupole Mass Spectrometer (Waters Corporation). The aniline-labeled HS digestion products were separated on an Acquity UPLC Glycan BEH Amide column (Waters Corporation) with a Glycan BEH Amide Pre-Column. Solvent A was acetonitrile. Solvent B was 100 mM ammonium formate in water, pH 4.5. The initial solvent composition was 80% A/20% B at a flow rate

of 0.2 ml/min. The column was kept at 50 °C. The LC elution gradient was as follows: 80% A/20% B for 0.5 min, ramped to 78.8% A/21.2% B over 5.5 min, then ramped to 62% A/38% B over 11 min, changed to 0% A/100% B for 7 min, and finally the column was re-equilibrated for 6 min at 80% A/20% B. Samples were ionized by electrospray ionization in the negative ion mode. The capillary voltage was set to 2.5 kV, the desolvation temperature was set to 300 °C, and the desolvation gas flow was 800 l/hr. One precursor–product ion transition was monitored for each of the HS residues (Table S3). Isobaric species were differentiated by retention times. A ratio of the amount of [$^{12}C_6$]-aniline-derivatized sample to the [$^{13}C_6$]-aniline-derivatized standard was used to determine the concentrations of the HS disaccharides and HS-NRE in each sample.

Brain scaling factors

Approximately 200 times from mouse (∼0.5 g) to Huntaway dog (∼100 g) (65) and 10 times from dog to juvenile human (∼1000 g).

Statistical tests

Statistical analysis was performed using one-way ANOVA of the log10 transformed data followed by Tukey's multiple comparisons test. For data with two factors, a two-way ANOVA with interaction of the log10 transformed data was performed, and if the interaction was significant, a Tukey's multiple comparison test was conducted.

Data availability

Data contained in the article are available from Eric Zanelli (eric@allievex.com) upon request.

Supporting information—This article contains supporting information.

Acknowledgments—The authors thank Allievex Corporation for their careful review and suggestions for this manuscript. The authors also thank Derek Janszen for help with the statistical analysis. The authors would also like to thank Steven Striepeke for the initial RP-HPLC purity assay method development and Lot 1 assessment, Philip Alferness for early rhSGSH N-glycan site occupancy and composition analysis, Vikas Bhat for early SEC-MALS evaluation, and Paul Fitzpatrick for purification management support. We also thank Biognosys for performing the proteomics work.

Author contributions—J. H. L., Stuart Bunting, Sherry Bullens, B. E. C., and J. C. W. conceptualization; J. M., S. J., B. B., V. A., H. W., A. G., L. M., B. H., C. V., M. P., N. Y., Y. Z., E. P., T. M. C., P. M. N. T., J. V., G. G., C. H., R. L., and J. C. W. methodology; L. M., B. H., C. V., and J. C. W. formal analysis; J. M., S. J., B. B., V. A., H. W., A. G., L. M., B. H., C. V., M. P., N. Y., Y. Z., E. P., I. S., O. G., A. A., M. J. L., S. A., J. V., and G. G. investigation; J. M., S. J., B. B., V. A., H. W., A. G., M. P., N. Y., Y. Z., E. P., I. S., M. J. L., S. A., J. V., G. G., and R. L. resources; L. M., B. H., C. V., S. F., R. L., and J. C. W. writing–original draft; J. M., V. A., H. W., L. M., B. H., C. V., M. P., N. Y., Y. Z., E. P., T. M. C., J. V., S. F., G. G., R. L., D. J. W., B. E. C., and J. C. W. writing–review and editing; J. M., L. M., B. H., C. V., and J. C. W. visualization; V. A., T. M. C., P. M. N. T., J. V., S. F., G. G., C. H., R. L., D. J. W., J. H. L., Stuart Bunting, Sherry Bullens, B. E. C., S. M. R., and J. C. W. supervision; H. W., B. H., J. V., S. M. R., and J. C. W. project administration; J. H. L., Stuart Bunting, Sherry Bullens, B. E. C., S. M. R., and J. C. W. funding acquisition.

Funding and additional information—This work was supported by BioMarin Pharmaceutical Inc.

Conflict of interest—The authors were employees of BioMarin Pharmaceutical Inc at the time of the studies. The authors declare that they have no conflicts of interest with the contents of this article.

Abbreviations—The abbreviations used are: CHO, Chinese hamster ovary; CNS, central nervous system; CSF, cerebrospinal fluid; ERT, enzyme replacement therapy; HS, heparan sulfate; h.e.d., human equivalent dose; HS-NRE, HS nonreducing end; ICV, intracerebroventricular; LC-PRM, liquid chromatography-parallel reaction monitoring; M6P, mannose-6-phosphate; MEF, mouse embryonic fibroblast; MPS, mucopolysaccharidosis; MS, mass spectrometry; rhSGSH, recombinant human SGSH; SEC, size-exclusion chromatography.

References

1. Neufeld, E. F., and Muenzer, J. (2019) The mucopolysaccharidoses. In: Valle, D. L., Antonarakis, S., Ballabio, A., Beaudet, A. L., Mitchell, G. A., eds. *The Online Metabolic and Molecular Bases of Inherited Disease*, McGraw-Hill, New York, NY
2. Truxal, K. V., Fu, H., McCarty, D. M., McNally, K. A., Kunkler, K. L., Zumberge, N. A., *et al.* (2016) A prospective one-year natural history study of mucopolysaccharidosis types IIIA and IIIB: implications for clinical trial design. *Mol. Genet. Metab.* **119**, 239–248
3. Shapiro, E. G., Nestrasil, I., Delaney, K. A., Rudser, K., Kovac, V., Nair, N., *et al.* (2016) A prospective natural history study of mucopolysaccharidosis type IIIA. *J. Pediatr.* **170**, 278–287
4. Valstar, M. J., Neijs, S., Bruggenwirth, H. T., Olmer, R., Ruijter, G. J. G., Wevers, R. A., *et al.* (2010) Mucopolysaccharidosis type IIIA: clinical spectrum and genotype-phenotype correlations. *Ann. Neurol.* **68**, 876–887
5. De Pasquale, V., and Pavone, L. M. (2019) Heparan sulfate proteoglycans: the sweet side of development turns sour in mucopolysaccharidoses. *Biochim. Biophys. Acta Mol. Basis Dis.* **1865**, 165539
6. Hemsley, K. M., King, B., and Hopwood, J. J. (2007) Injection of recombinant human sulfamidase into the CSF via the cerebellomedullary cistern in MPS IIIA mice. *Mol. Genet. Metab.* **90**, 313–328
7. Hemsley, K. M., Beard, H., King, B. M., and Hopwood, J. J. (2008) Effect of high dose, repeated intra-cerebrospinal fluid injection of sulphamidase on neuropathology in mucopolysaccharidosis type IIIA mice. *Genes Brain Behav.* **7**, 740–753
8. Hemsley, K. M., Luck, A. J., Crawley, A. C., Hassiotis, S., Beard, H., King, B., *et al.* (2009) Examination of intravenous and intra-CSF protein delivery for treatment of neurological disease. *Eur. J. Neurosci.* **29**, 1197–1214
9. Beard, H., Luck, A. J., Hassiotis, S., King, B., Trim, P. J., Snel, M. F., *et al.* (2015) Determination of the role of injection site on the efficacy of intra-CSF enzyme replacement therapy in MPS IIIA mice. *Mol. Genet. Metab.* **115**, 33–40
10. Beard, H., Hassiotis, S., Luck, A. J., Rozaklis, T., Hopwood, J. J., and Hemsley, K. M. (2016) Continual low-dose infusion of sulfamidase is superior to intermittent high-dose delivery in ameliorating neuropathology in the MPS IIIA mouse brain. *JIMD Rep.* **29**, 59–68
11. King, B., Hassiotis, S., Rozaklis, T., Beard, H., Trim, P. J., Snel, M. F., *et al.* (2016) Low-dose, continuous enzyme replacement therapy ameliorates brain pathology in the neurodegenerative lysosomal disorder mucopolysaccharidosis type IIIA. *J. Neurochem.* **137**, 409–422

12. Marshall, N. R., Hassiotis, S., King, B., Rozaklis, T., Trim, P. J., Duplock, S. K., *et al.* (2015) Delivery of therapeutic protein for prevention of neurodegenerative changes: comparison of different CSF-delivery methods. *Exp. Neurol.* **263**, 79–90
13. King, B., Marshall, N., Beard, H., Hassiotis, S., Trim, P. J., Snel, M. F., *et al.* (2015) Evaluation of enzyme dose and dose-frequency in ameliorating substrate accumulation in MPS IIIA Huntaway dog brain. *J. Inherit. Metab. Dis.* **38**, 341–350
14. King, B., Marshall, N. R., Hassiotis, S., Trim, P. J., Tucker, J., Hattersley, K., *et al.* (2017) Slow, continuous enzyme replacement via spinal CSF in dogs with the pediatric-onset neurodegenerative disease, MPS IIIA. *J. Inherit. Metab. Dis.* **40**, 443–453
15. Fraldi, A., Hemsley, K., Crawley, A., Lombardi, A., Lau, A., Sutherland, L., *et al.* (2007) Functional correction of CNS lesions in an MPS-IIIA mouse model by intracerebral AAV-mediated delivery of sulfamidase and SUMF1 genes. *Hum. Mol. Genet.* **16**, 2693–2702
16. Ruzo, A., Marcö, S., García, M., Villacampa, P., Ribera, A., Ayuso, E., *et al.* (2012) Correction of pathological accumulation of glycosaminoglycans in central nervous system and peripheral tissues of MPSIIIA mice through systemic AAV9 gene transfer. *Hum. Gene Ther.* **23**, 1237–1246
17. Haurigot, V., Marcó, S., Ribera, A., Garcia, M., Ruzo, A., Villacampa, P., *et al.* (2013) Whole body correction of mucopolysaccharidosis IIIA by intracerebrospinal fluid gene therapy. *J. Clin. Invest.* **123**, 3254–3271
18. Duncan, F. J., Naughton, B. J., Zaraspe, K., Murrey, D. A., Meadows, A. S., Clark, K. R., *et al.* (2015) Broad functional correction of molecular impairments by systemic delivery of scAAVrh74-hSGSH gene delivery in MPS IIIA mice. *Mol. Ther.* **23**, 638–647
19. Fu, H., Cataldi, M. P., Ware, T. A., Zaraspe, K., Meadows, A. S., Murrey, D. A., *et al.* (2016) Functional correction of neurological and somatic disorders at later stages of disease in MPS IIIA mice by systemic scAAV9-hSGSH gene delivery. *Mol. Ther. Methods Clin. Dev.* **3**, 16036–16047
20. Winner, L. K., Beard, H., Hassiotis, S., Lau, A. A., Luck, A. J., Hopwood, J. J., *et al.* (2016) A preclinical study evaluating AAVrh10-based gene therapy for Sanfilippo syndrome. *Hum. Gene Ther.* **27**, 363–375
21. Maccari, F., Sorrentino, N. C., Mantovani, V., Galeotti, F., Fraldi, A., and Volpi, N. (2017) Glycosaminoglycan levels and structure in a mucopolysaccharidosis IIIA mice and the effect of a highly secreted sulfamidase engineered to cross the blood-brain barrier. *Metab. Brain Dis.* **32**, 203–210
22. Tardieu, M., Zérah, M., Husson, B., de Bournonville, S., Deiva, K., Adamsbaum, C., *et al.* (2014) Intracerebral administration of adeno-associated viral vector serotype rh.10 carrying human SGSH and SUMF1 cDNAs in children with mucopolysaccharidosis type IIIA disease: results of a phase I/II trial. *Hum. Gene Ther.* **25**, 506–516
23. Gustaavsson, S., Sjöström, E. O., Tjernberg, A., Janson, J., Westermark, U., Andersson, T., *et al.* (2019) Intravenous delivery of a chemically modified sulfamidase efficiently reduces heparan sulfate storage and brain pathology in mucopolysaccharidosis IIIA mice. *Mol. Genet. Metab. Rep.* **21**, 100510
24. Sorrentino, N. C., D'Orsi, L., Sambri, I., Nusco, E., Monaco, C., Spampanato, C., *et al.* (2013) A highly secreted sulphamidase engineered to cross the blood-brain barrier corrects brain lesions of mice with mucopolysaccharidoses type IIIA. *EMBO Mol. Med.* **5**, 675–690
25. Lawrence, R., Brown, J. R., Lorey, F., Dickson, P. I., Crawford, B. E., and Esko, J. D. (2014) Glycan-based biomarkers for mucopolysaccharidoses. *Mol. Genet. Metab.* **111**, 73–83
26. Jones, S. A., Breen, C., Heap, F., Rust, S., de Ruijter, J., Tump, E., *et al.* (2016) A phase 1/2 study of intrathecal heparan-N-sulfatase in patients with mucopolysaccharidosis IIIA. *Mol. Genet. Metab.* **118**, 198–205
27. Wijburg, F. A., Whitley, C. B., Muenzer, J., Gasperini, S., del Toro, M., Muschol, N., *et al.* (2019) Intrathecal heparan-N-sulfatase in patients with Sanfilippo syndrome type A: a phase IIB randomized trial. *Mol. Genet. Metab.* **126**, 121–130
28. Aoyagi-Scharber, M., Crippen-Harmon, D., Lawrence, R., Vincelette, J., Yogalingam, G., Prill, H., *et al.* (2017) Clearance of heparan sulfate and attenuation of CNS pathology by intracerebroventricular BMN 250 in Sanfilippo type B mice. *Mol. Ther. Methods Clin. Dev.* **6**, 43–53
29. Kornfeld, S. (1992) Structure and function of the mannose 6-phosphate/insulin-like growth factor II receptors. *Annu. Rev. Biochem.* **61**, 307–330
30. Gliddon, B. L., Yogalingam, G., and Hopwood, J. J. (2004) Purification and characterization of recombinant murine sulfamidase. *Mol. Genet. Metab.* **83**, 239–245
31. Bielicki, J., Hopwood, J. J., Melville, E. L., and Anson, D. S. (1998) Recombinant human sulphamidase: expression, amplification, purification and characterization. *Biochem. J.* **329**, 145–150
32. Natale, P. D., Vanacore, B., Daniele, A., and Esposito, S. (2001) Heparan N-sulfatase: in vitro mutagenesis of potential N-glycosylation sites. *Biochem. Biophys. Res. Commun.* **280**, 1251–1257
33. Chen, Y., Zheng, S., Tecedor, L., and Davidson, B. (2018) Overcoming limitations inherent in sulfamidase to improve mucopolysaccharidosis IIIA gene therapy. *Mol. Ther.* **26**, 1118–1126
34. Staudt, C., Puissant, E., and Boonen, M. (2017) Subcellular trafficking of mammalian lysosomal proteins: an extended view. *Int. J. Mol. Sci.* **18**, 47
35. Bu, G. (2001) The roles of receptor-associated protein (RAP) as a molecular chaperone for members of the LDL receptor family. *Int. Rev. Cytol.* **209**, 79–116
36. Willnow, T. E., and Herz, J. (1994) Genetic deficiency in low density lipoprotein receptor-related protein confers cellular resistance to *Pseudomonas* exotoxin A. *J. Cell Sci.* **107**, 719–726
37. Zhang, Y., Huo, M., Zhou, J., and Xie, S. (2010) PKSolver: an add-in program for pharmacokinetic and pharmacodynamics data analysis in Microsoft excel. *Comput. Methods Programs Biomed.* **99**, 306–314
38. Passaro, A. P., Lebos, A. L., Yao, Y., and Stice, S. L. (2021) Immune response in neurological pathology: emerging role of central and peripheral immune crosstalk. *Front. Immunol.* **12**, 676621
39. Hol, E. M., and Pekny, M. (2015) Glial fibrillary acidic protein (GFAP) and the astrocyte intermediate filament system in diseases of the central nervous system. *Curr. Opin. Cell Biol.* **32**, 121–130
40. Terryn, J., Verfaillie, C. M., and Van Damme, P. (2021) Tweaking progranulin expression: therapeutic avenues and opportunities. *Front. Mol. Neurosci.* **14**, 713031
41. Schartz, N. D., and Tenner, A. J. (2020) The good, the bad, and the opportunities of the complement system in neurodegenerative disease. *J. Neuroinflammation* **17**, 354
42. Auderset, L., Cullen, C. L., and Young, K. M. (2016) Low density lipoprotein-receptor related protein 1 is differentially expressed by neuronal and glial populations in the developing and mature mouse central nervous system. *PLoS One* **11**, e0155878
43. Prasad, J., Young, P. A., and Strickland, D. K. (2016) High affinity binding of the receptor-associated protein D1D2 domains with the low density lipoprotein receptor-related protein (LRP1) involves bivalent complex formation. *J. Biol. Chem.* **291**, 18430–18439
44. Liu, Y., Jones, M., Hingtgen, C. M., Bu, G., Laribee, N., Tanzi, R. E., *et al.* (2000) Uptake of HIV-1 Tat protein mediated by low-density lipoprotein receptor-related protein disrupts the neuronal metabolic balance of the receptor ligands. *Nat. Med.* **6**, 1380–1387
45. Okada, Y., Yamada, S., Toyoshima, M., Dong, J., Nakajima, M., and Sugahara, K. (2002) Structural recognition by recombinant human heparanase that plays critical roles in tumor metastasis. *J. Biol. Chem.* **277**, 42488–42495
46. Griffin, L. S., and Gloster, T. M. (2017) The enzymatic degradation of heparan sulfate. *Protein Pet. Lett.* **24**, 710–722
47. Naimy, H., Powell, K. D., Moriarity, J. R., Wu, J., McCauley, T. G., Haslett, P. A. J., *et al.* (2016) A novel LC-MS/MS assay for heparan sulfate screening in the cerebrospinal fluid of mucopolysaccharidosis IIIA patients. *Bioanalysis* **8**, 285–295
48. Tanaka, N., Kida, S., Kinoshita, M., Morimoto, H., Shibasaki, T., Tachibana, K., *et al.* (2018) Evaluation of cerebrospinal fluid heparan sulfate as a biomarker of neuropathology in a murine model of mucopolysaccharidosis type II using high-sensitivity LC/MS/MS. *Mol. Genet. Metab.* **125**, 53–58
49. Sands, M. S., Vogler, C., Torrey, A., Levy, B., Gwynn, B., Grubb, J., *et al.* (1997) Murine mucopolysaccharidosis type VII: long term therapeutic effects of enzyme replacement and enzyme replacement followed by bone marrow transplantation. *J. Clin. Invest.* **99**, 1596–1605

50. Jolly, R. D., Marshall, N. R., Perrott, M. R., Dittmer, K. E., Hemsley, K. M., and Beard, H. (2011) Intracisternal enzyme replacement therapy in lysosomal storage diseases: routes of absorption into brain. *Neuropathol. Appl. Neurobiol.* **37**, 414–422
51. Kan, S., Aoyagi-Scharber, M., Le, S. Q., Vincelette, J., Ohmi, K., Bullens, S., *et al.* (2014) Delivery of an enzyme-IGFII fusion protein to the mouse brain is a therapeutic for mucopolysaccharidosis type IIIB. *Proc. Natl. Acad. Sci. U. S. A.* **111**, 14870–14875
52. Vogler, C., Sands, M., Higgins, A., Levy, B., Grubb, J., Birkenmeier, E. H., *et al.* (1993) Enzyme replacement with recombinant beta-glucuronidase in the newborn mucopolysaccharidosis type VII mouse. *Pediatr. Res.* **34**, 837–840
53. Ellinwood, N. M., Valentine, B., Hess, A. S., Jens, J. K., Snella, E. M., Ware, W. A., *et al.* (2018) Pharmacology of BMN 250 administered via intracerebroventricular infusion once every 2 weeks for twenty-six weeks or longer in a canine model of mucopolysaccharidosis type IIIB. *Mol. Genet. Metab.* **123**, S42
54. Lin, S., Cleary, M., Couce, M. L., De Castro Lopez, M. J., Harmatz, P., Lee, J., *et al.* (2018) ICV-administered BMN 250 is well tolerated and reduces heparan sulfate accumulation in the CNS of subjects with Sanfilippo Syndrome Type B. *J. Inherit. Metab. Dis.* **41**, S168–S169
55. Cleary, M., Muschol, N., Couce, M. L., Harmatz, P., Lee, J., Lin, S., *et al.* (2019) ICV-administered tralesinidase alfa (BMN 250 NAGLU-IGF2) is well-tolerated and reduces heparan sulfate accumulation in the CNS of subjects with Sanfilippo syndrome type B (MPS IIIB). *Mol. Genet. Metab.* **126**, S40
56. Bhaumik, M., Muller, V. J., Rozaklis, T., Johnson, L., Dobrenis, K., Bhattacharyya, R., *et al.* (1999) A mouse model for mucopolysaccharidosis type III A (Sanfilippo syndrome). *Glycobiology* **9**, 1389–1396
57. Crawley, A. C., Gliddon, B. L., Auclair, D., Brodie, S. L., Hirte, C., King, B. M., *et al.* (2006) Characterization of a C57BL/6 congenic mouse strain of mucopolysaccharidosis type IIIA. *Brain Res.* **1104**, 1–17
58. Szabo, Z., Guttman, A., Rejtar, T., and Karger, B. L. (2010) Improved sample preparation method for glycan analysis of glycoproteins by CE-LIF and CE-MS. *Electrophoresis* **31**, 1389–1395
59. Bhattacharyya, R., Gliddon, B., Beccari, T., Hopwood, J. J., and Stanley, P. (2001) A novel missense mutation in lysosomal sulfamidase is the basis of MPS III A in a spontaneous mouse mutant. *Glycobiology* **11**, 99–103
60. Schindelin, J., Arganda-Carreras, I., Frise, E., Kaynig, V., Longair, M., Pietzsch, T., *et al.* (2012) Fiji: an open-source platform for biological-image analysis. *Nat. Methods*, 676–682
61. Escher, C., Reiter, L., BacLean, B., Ossola, R., Herzog, F., Chilton, J., *et al.* (2012) Using iRT, a normalized retention time for more targeted measurement of peptides. *Proteomics* **12**, 1111–1121
62. Reiter, L., Rinner, O., Picotti, P., Hüttenhain, R., Beck, M., Brusniak, M., *et al.* (2011) mProphet: automated data processing and statistical validation for large-scale SRM experiments. *Nat. Methods* **8**, 430–435
63. Lawrence, R., Olson, S. K., Steele, R. E., Wang, L., Warrior, R., Cummings, R. D., *et al.* (2008) Evolutionary differences in glycosaminoglycan fine structure detected by quantitative glycan reductive isotope labeling. *J. Biol. Chem.* **283**, 33674–33684
64. Lawrence, R., Brown, J. R., Al-Mafraji, K., Lamanna, W. C., Beitel, J. R., Boons, G. J., *et al.* (2012) Disease-specific non-reducing end carbohydrate biomarkers for mucopolysaccharidoses. *Nat. Chem. Biol.* **8**, 197–204
65. Bronson, R. T. (1979) Brain weight-body weight scaling in breeds of dogs and cats. *Brain Behav. Evol.* **16**, 227–236